ROYAL SOCIETY
OF CHEMISTRY

COMMUNICATION

Check for updates

Disulfide exchange assisted self-healing epoxy/PDMS/graphene oxide nanocomposites†

Balaji Krishnakumar,[a] Manjeet Singh,[a] Vijay Parthasarthy,[a] Chanwook Park,[b] Nanda Gopal Sahoo, [ID][c] Gun Jin Yun*[b] and Sravendra Rana [ID]*[a]

Vitrimers, a class of polymeric networks that change their topology above a threshold temperature, have been investigated in recent years. In order to further extend their properties, in this research, we demonstrate disulfide exchange assisted polydimethylsiloxane (PDMS)- and graphene oxide (GO)-involved epoxy vitrimers, which exhibit a reduction in glass transition temperature and storage modulus with increase in flexural strain and low-temperature self-healing. Stress relaxation and Arrhenius study were carried out for the analysis of vitrimeric behavior, where the prepared epoxy material displays self-healing at 80 °C for 5 min, whereas a low-temperature self-healing (60 °C) was observed for epoxy/PDMS/GO nanocomposites.

Introduction

Thermoset materials with excellent mechanical,[1–3] thermal[4] and chemical resistance properties[5] have been developed for many industrial,[6] aircraft,[7] wind turbine[8] and composite applications.[9] However, due to the lack of re-processability, recyclability, and reshaping ability, their applications have been restricted.[10] In contrast, some thermoplastic materials have the ability to flow in certain temperature ranges and this prevailing temperature response is intriguing in reprocessing. However, their lower strength and structural ability do not match the required properties.[11,12] Recyclable/reprocessable thermoset polymers have emerged over the past few years to acquire reliable reprocessing through simple and efficient mechanisms.[13,14] In particular dynamic covalent exchange promoted thermoset

[a]University of Petroleum & Energy Studies (UPES), School of Engineering, Energy Acres, Bidholi, Dehradun, 248007, India. E-mail: srana@ddn.upes.ac.in

[b]Institute of Advanced Aerospace Technology, Seoul National University, Gwanak-ro 1, Gwanak-gu, Seoul 08826, South Korea. E-mail: gunjin.yun@snu.ac.kr

[c]Nanoscience and Nanotechnology Centre, Department of Chemistry, Kumaun University, D.B.S. Campus, Nainital, Uttarakhand, 263001, India

† Electronic supplementary information (ESI) available. See DOI: 10.1039/d0na00282h

materials were demonstrated with recycling and self-healing behavior,[15–20] where during reprocessing promising associative exchange results in a concurrent exchange between chains, as introduced by Leibler and coworkers.[21] The reported epoxy vitrimers execute associative exchanges through transesterification reactions, and the role of catalysts in exchange reactions was investigated thoroughly.[22] Since then, many reports have discussed vitrimer materials with different chemistries such as transesterification,[23–26] transalkylation,[27] transamination,[28] disulfide,[29–31] transcarbamoylation[32,33] and transcarbonation.[34] Among these reactions, disulfide exchanges were prominently discussed in self-healing studies to realize effective properties.[35,36]

In the present study, catalyst-free disulfide exchange-promoted epoxy/PDMS/GO nanocomposite vitrimer materials with self-healing behavior are reported. The addition of catalyst not only causes toxicity but the mixing challenge also compromises the mechanical properties of the synthesized vitrimers. In addition, dynamic bond-exchange reactions often occur at elevated temperature, and thermal degradation could be hastened in the presence of a catalyst. Therefore, the absence of catalyst is advantageous owing to non-toxicity and non-degradability at high temperature.[37,38] Furthermore, the addition of PDMS should not only be helpful for achieving low-temperature self-healing, but would also be helpful to overcome the brittleness of the epoxy matrix and improve its impact properties, including the resistance to crack propagation. As covalently crosslinked pristine epoxy demonstrates a brittle failure, the involvement of flexible epoxy-terminated PDMS has been effectuated to increase the toughness,[39,40] and the incorporation of GO is helpful to enhance the material strength. The prepared composite vitrimer material exhibits a reduction in glass transition temperature (T_g) and storage modulus including an enhancement in flexural strain. The mechanical strength was increased by the addition of GO nanofillers, and fine dispersion of PDMS and GO was evaluated through SEM and contact angle measurements. Furthermore, vitrimer behavior was observed through stress relaxation characteristics

and Arrhenius plots. The prepared pristine epoxy (EP-p) material displays self-healing at 80 °C for 5 min, whereas a low-temperature self-healing (60 °C) was observed for epoxy/PDMS/GO nanocomposites.

Experimental section

Materials and methods

Bisphenol A diglycidyl ether (BADGE) (340.41 g mol^{-1}) resin, diglycidyl ether terminated PDMS (800 g mol^{-1}), 2-aminophenyl disulfide (2-AFD) (248.37 g mol^{-1}) hardener and graphite flakes were purchased from Sigma-Aldrich.

Preparation of epoxy composites

In a round-bottom flask, BADGE resin and epoxy terminated PDMS were stirred at 130 °C for 7 hours, and later 2-AFD was added and the reaction mixture was continuously stirred at the same temperature for 15 min (Fig. 1). Subsequently, the reaction mixture was poured into a mold and kept at 150 °C for 5 hours for curing. Finally, the attained specimen was used for further studies including those of mechanical and self-healing properties. To optimize the PDMS effect in epoxy, different percentages of PDMS were incorporated in the matrix and investigated effectively (shown in Table 1), and the samples were denoted as EP-x% (x = p (0), 1, 2, 3 and 5) (Table S1(a)†).

Preparation of epoxy nanocomposites

A similar procedure was followed for the preparation of nanocomposites, where ethanol-dispersed GO solution was added (Table S1(b)†) in the mixture (PDMS/epoxy) and stirring continued until ethanol evaporation. Finally, 2-AFD was added and stirred for another 15 min. The reaction mixture was poured in a mold and kept in an oven at 150 °C for 5 h.

Characterization techniques

GO was prepared through the Hummers method[41,42] (SI) from graphite flakes. The obtained X-ray diffraction (D8 ADVANCE ECO, Bruker) peak shifting from 23° (graphite) to 12.3° confirmed the GO formation (Fig. S1†). FTIR (Frontier FT-IR/FIR, PerkinElmer) analysis was used for characterization. Rectangular specimens (15 mm × 5 mm × 0.5 mm) were

Table 1 Glass transition temperature and contact angle values of different samples

Epoxy/PDMS (EP-x)	Glass transition temperature (T_g)	Contact angle (°)
EP-p	64	85
EP-1	62	88
EP-2	58	97
EP-3	62	94
EP-5	63	89
Epoxy–PDMS–GO (EP-2-y)		
EP-2-0.1	57	98
EP-2-0.2	56	99
EP-2-0.5	53	101
EP-2-1	55	97
EP-2-2	58	97

investigated by TA-Q400em three-point bending test (40 °C to 120 °C) to determine the storage modulus and loss modulus (heat rate of 10 °C min^{-1}; 50 mL min^{-1} nitrogen; 0.02 N). Stress relaxation and stress–strain experiments were performed at 40 °C, with 1 × 10^{-3} N preload (1% strain) and 0.02 N force respectively.

Results and discussion

The curing of epoxy was examined over regular time intervals (hourly basis) with the help of FTIR analysis (Fig. S2†); eventually after 5 hours no decrease (914 cm^{-1}) was observed (Fig. 2(a)).[36] Furthermore, THF swelling test was performed to identify the complete curing, as uncured epoxy-PDMS composite had unbonded covalent formations, which could not be retained under vigorous stirring (Fig. S3†). The dispersion of PDMS in epoxy was investigated through contact angle and SEM analysis. Initially, dispersion of the PDMS in epoxy was evaluated with hydrophobic changes, where enhancement in hydrophobicity was observed [sample EP-2], which could be due to a good dispersion of PDMS in epoxy matrix.[40,43] However, with further addition of PDMS a gradual decrease in hydrophobicity
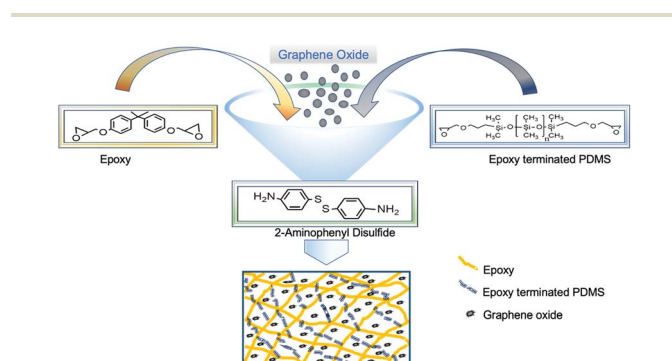

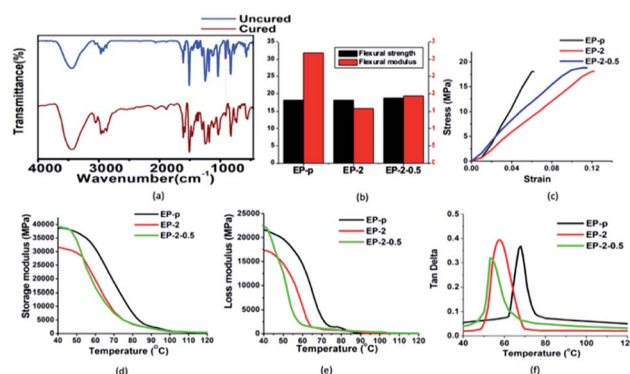Fig. 1 Synthesis route of epoxy-PDMS-GO nanocomposite.

Fig. 2 (a) FTIR spectra. (b) Bar diagram for flexural strength and modulus of different samples. (c) Stress–strain, (d) storage modulus, (e) loss modulus and (f) tan δ.

was observed (Table 1), denoting PDMS dispersion failure in the matrix.[40] A similar kind of behavior was observed for GO-based composites, where hydrophobicity was increased with incorporation of GO [EP-2-0.5], whereas further increasing GO incorporation decreases the hydrophobicity (Table 1). The temperature-dependent transition was noticed through DMA analysis and the obtained glass transition temperatures of the epoxy vitrimer samples are tabulated in Table 1. The resulting glass transition temperature effectively indicated that the incorporation of PDMS and GO is advantageous to reduce the T_g of the prepared composites. The observed change in T_g behavior could be owing to (i) low T_g of PDMS[44] or (ii) fine dispersion of PDMS.[43] However, after further addition of PDMS an increase in T_g was obtained.

To find out the impact of nanofillers, different percentages of GO were included in EP-2 samples, and the obtained results demonstrate a further decrease in T_g, where GO-based nanofillers exhibit a free volume space between matrix and filler.[45] However, a further addition of GO increases the T_g of the composites [EP-2-1; EP-2-2], which might be again due to agglomeration of GO, thus leading to poor interaction with the epoxy-PDMS matrix.

Based on these observations, further investigations were carried out for EP-p, EP-2 and EP-2-0.5 specimens. The determined storage modulus (E'), loss modulus (E'') and tan δ data exhibit a temperature-dependent viscoelastic behavior (Fig. 2(d–f)) for the prepared specimens and the obtained storage modulus of EP-p at 40 °C was much higher than that of EP-2. The reduction in storage modulus could be due to the presence of PDMS, which demonstrates a lower crosslinking density.[43]

Furthermore, incorporated GO restrains the covalent formation of epoxy and thus leads to the free volume space between filler and matrix. The storage modulus of specimen EP-2-0.5 was higher than that of EP-2, which could be due to the wavy topology of GO, enhancing intercalate interlocking between matrix and nanofiller at low temperature.[46]

Stress–strain curve shows that flexural strength (Fig. 2(b)) of Ep-p (18 MPa) was slightly lower than that of EP-2 and EP-2-0.5 (18.1 MPa and 18.7 MPa, respectively), though EP-2 strain at break point was higher than that of EP-p and EP-2-0.5 (Fig. 2(c)). The observed strain at break increase exemplified the flexural modulus decrease, and thus acquired due to the presence of PDMS which reduces the bending resistance/brittleness. Substantially, observed strain at break values of EP-2 and Ep-
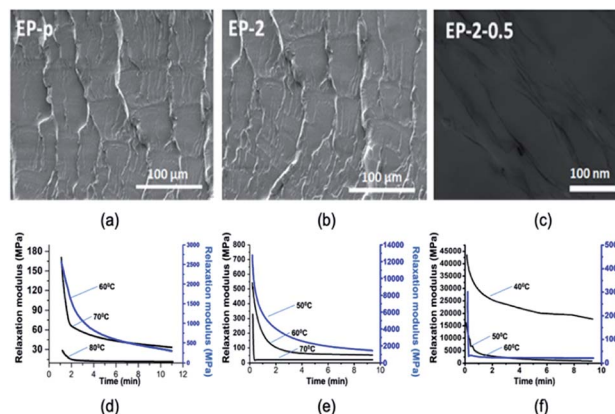

Fig. 3 (a) SEM image of EP-p. (b) SEM image of epoxy/PDMS. (c) TEM image of epoxy/PDMS/GO nanocomposite. Stress relaxation analysis at different temperatures for (d) EP-p, (e) EP-2 and (f) EP-2-0.5.

2-0.5 have increased two times (from 0.06 to 0.12) and 50% (0.06 to 0.09) compared to EP-p, respectively, whereas the obtained flexural moduli of EP-2 and EP-2-0.5 (15.7 GPa and 19.4 GPa, respectively) were less than the EP-p flexural modulus (32.1 GPa) (shown in Table 2).

SEM analysis was carried out to study the effect of PDMS in the epoxy matrix. The fractured surfaces in Fig. 3(a and b) show that there is a homogeneous cured resin as no phase domains could be observed. The dispersibility of the GO nanosheets was analyzed using TEM imaging (Fig. 3(c)).

The images show an excellent dispersion of GO nanosheets in epoxy vitrimer matrix (EP-2). For identifying the vitrimer behavior, stress relaxation behavior of the materials was studied.[36] For instance, relaxation times of 112.8 s, 40.8 s and 34 s at 60 °C, 70 °C and 80 °C, respectively, were observed for EP-p specimen (Fig. 3(d)). However, in the case of EP-2, relaxation times of 42.6 s, 27.6 s and 13.8 s at 50 °C, 60 °C and 70 °C respectively were observed (Fig. 3(e)). However, due to the faster relaxation after T_g, specimen EP-2-0.5 demonstrates times of 89.6 s, 16.8 s and 3 s at 40 °C, 50 °C and 60 °C, respectively (Fig. 3(f)). Thus, obtained relaxation times were plotted on a graph to identify the Arrhenius equation, and from that equation activation energy (E_a) was calculated (Table 2). The material T_v has been generally considered once the viscosity reaches 10^{12} Pa s;[21] hence this hypothesized T_v temperature range has been extrapolated based on the literature[36] (see ESI†)

Table 2 Different properties of EP-p, EP-2 and EP-2-0.5 samples

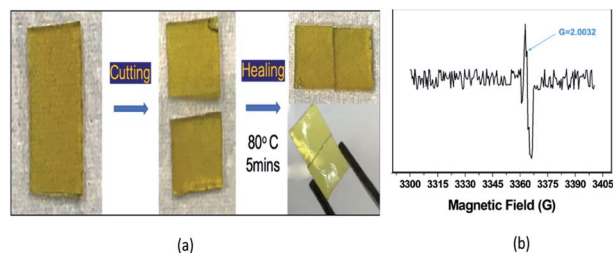| Sample	Storage modulus (GPa)	Flexural strength (MPa)	Flexural strain at break (mm mm^{-1})	Flexural modulus (GPa)	Activation energy (E_a) (kJ mol^{-1})	Topology transition temperature (T_v) (°C)	Before healing (GPa)	After healing (GPa)	
								1st	2nd
EP-p	39.7	18.0	0.06	32.1	59	19	32.1	23.4	19.5
EP-2	31.6	18.1	0.12	15.7	52	−1	15.7	13.5	12.1
EP-2-0.5	39.9	18.7	0.09	19.4	180	31	19.4	17.3	15.8

Fig. 4 (a) Healing of sample EP-2. (b) EPR analysis graph.

for EP-p sample. Subsequently, investigated low-viscosity siloxanes containing PDMS involved in EP-2 resulted in a lower activation energy (E_a)[47] and T_v than EP-p (Table 2).[44,48]

However, owing to the presence of GO, EP-2-0.5 exhibits a higher T_v and E_a than EP-2 (not EP-p), where GO nanofiller leads to an increase in viscosity and thus restricts the low-temperature chain mobility,[49] whereas assimilated free volume has reduced the T_g.[45] Self-healing behavior of EP-p was observed at 80 °C for 5 min, whereas the EP-2 and EP-2-0.5 samples demonstrate efficient healing at 60 °C for 5 min, which could be due to their lower T_g. The obtained self-healing of the material was acquired through disulfide exchanges, where sulfide radicals were accumulated at certain temperature (Fig. 4(a)). Such sulfide radical exchanges have been identified through electron paramagnetic resonance (EPR) analysis (80 °C) and the observed (g value = 2.003) peak confirms the radical formation in the material (Fig. 4(b)).

Further, the self-healing efficiency was evaluated through the flexural modulus, where the strength of the material was found to be almost the same after consecutive healing (Table 2). The observed healing efficiency of the material was addressed through flexural modulus changes, where healing efficiencies of 72%, 85%, and 89% in the first cycle and 60%, 77%, and 82% in

the second cycle were observed for EP-p, EP-2 and EP-2-0.5 specimens respectively (Fig. 5).

Conclusions

The synthesized epoxy-PDMS composite material exhibits a prominent reduction in glass transition temperature and effective decrease in bending resistance; however, the strength of the material does not show any change. After addition of PDMS and GO nanofiller in the epoxy vitrimer, certain mechanical properties were investigated through flexural studies and the obtained results indicated a difference in mechanical strength, strain at break and modulus. The pristine epoxy (EP-p) specimen demonstrates healing behavior at 80 °C for 5 min, whereas specimens EP-2 and EP-2-0.5 demonstrate healing at 60 °C for 5 min. Furthermore, the analyzed flexural modulus is helpful to quantify the mechanical properties and healing efficiency, where reduction in flexural modulus was observed after each healing cycle. However, the flexural strength of the material was not changed after two successive healing cycles. Overall, vitrimeric materials have enriched polymeric research *via* symbiosis of thermoset and thermoplastic properties. However, the demonstrated high glass transition temperature and activation energy restrict their performances. To overcome those snags, different mechanisms are involved. Herein, the synthesized multifunctional epoxy/PDMS/GO nanocomposite provides a new pathway to achieve a low glass transition temperature, required/designed to obtain a low-temperature self-healing, which is a current focus of interest.

Conflicts of interest

There is no conflict of interest.

Acknowledgements

Fig. 5 Stress−strain curves for (a) EP-p, (b) EP-2 and (c) EP-2-0.5 and (d) bar diagram for changes in flexural modulus after two healing cycles.

References

1 A. Shiota and C. K. Ober, *Prog. Polym. Sci.*, 1997, **22**, 975–1000.

2 A. Tcharkhtchi, S. Faivre, L. E. Roy, J. P. Trotignon and J. Verdu, *J. Mater. Sci.*, 1996, **31**, 2687–2692.

3 M. J. Mullins, D. Liu and H.-J. Sue, in *Thermosets*, ed. Q. Guo, Woodhead Publishing, 2012, pp. 28–61.

4 D. Ratna, in *Thermosets*, ed. Q. Guo, Woodhead Publishing, 2012, pp. 62–91.

5 *Chemical Resistance of Thermosets*, ed. E. Baur, K. Ruhrberg and W. Woishnis, William Andrew Publishing, 2018, pp. i–iii.
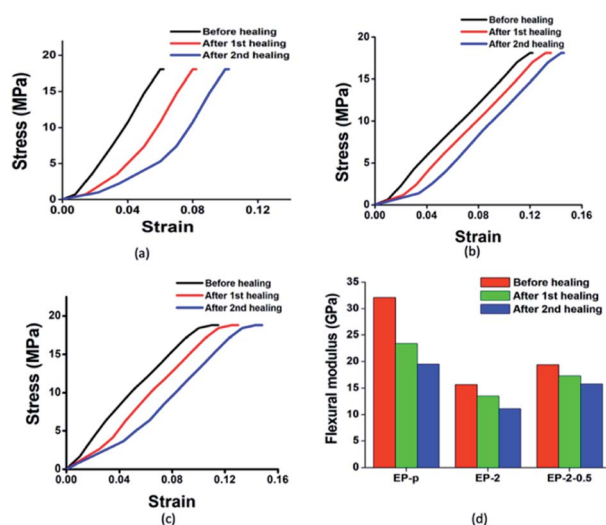
6 D. Song and R. K. Gupta, in *Thermosets*, ed. Q. Guo, Woodhead Publishing, 2012, pp. 165–188.

7 J. Baur and E. Silverman, *MRS Bull.*, 2007, **32**, 328–334.

8 L. Mishnaevsky, K. Branner, H. N. Petersen, J. Beauson, M. McGugan and B. F. Sørensen, *Materials*, 2017, **10**, 1–24.

9 C. T. Murray, R. L. Rudman, M. B. Sabade and A. V. Pocius, *MRS Bull.*, 2003, **28**, 449–454.

10 A. Cervenka, in *Mechanics of Composite Materials and Structures*, ed. C. A. M. Soares, C. M. M. Soares and M. J. M. Freitas, Springer Netherlands, Dordrecht, 1999, pp. 289–298.

11 J. D. Muzzy and A. O. Kays, *Polym. Compos.*, 1984, **5**, 169–172.

12 G. Ken, *Microelectron. Int.*, 1999, **16**, 34–38.

13 A. Li, J. Fan and G. Li, *J. Mater. Chem. A*, 2018, **6**, 11479–11487.

14 Y. Zhang, H. Ying, K. R. Hart, Y. Wu, A. J. Hsu, A. M. Coppola, T. A. Kim, K. Yang, N. R. Sottos, S. R. White and J. Cheng, *Adv. Mater.*, 2016, **28**, 7646–7651.

15 K. R. Hart, E. D. Wetzel, N. R. Sottos and S. R. White, *Composites, Part B*, 2019, **173**, 106808.

16 L. Guadagno, L. Vertuccio, C. Naddeo, E. Calabrese, G. Barra, M. Raimondo, A. Sorrentino, W. H. Binder, P. Michael and S. Rana, *Polymers*, 2019, **11**, 903.

17 M. Odarczenko, D. Thakare, W. Li, S. P. Venkateswaran, N. R. Sottos and S. R. White, *Adv. Eng. Mater.*, 2020, **22**, 1901223.

18 R. V. S. P. Sanka, B. Krishnakumar, Y. Leterrier, S. Pandey, S. Rana and V. Michaud, *Front. Mater.*, 2019, **6**, 137.

19 S. Chen, N. Mahmood, M. Beiner and W. H. Binder, *Angew. Chem., Int. Ed.*, 2015, **54**, 10188–10192.

20 S. Y. Kim, N. R. Sottos and S. R. White, *Compos. Sci. Technol.*, 2019, **175**, 122–127.

21 D. Montarnal, M. Capelot, F. Tournilhac and L. Leibler, *Science*, 2011, **334**, 965–968.

22 B. Krishnakumar, R. V. S. P. Sanka, W. H. Binder, V. Parthasarthy, S. Rana and N. Karak, *Chem. Eng. J.*, 2019, 123820.

23 H. Han and X. Xu, *J. Appl. Polym. Sci.*, 2018, **135**, 46307.

24 H. Zhang, C. Cai, W. Liu, D. Li, J. Zhang, N. Zhao and J. Xu, *Sci. Rep.*, 2017, **7**, 1–9.

25 Z. Yang, Q. Wang and T. Wang, *ACS Appl. Mater. Interfaces*, 2016, **8**, 21691–21699.

26 R. Long, H. J. Qi and M. L. Dunn, *Soft Matter*, 2013, **9**, 4083–4096.

27 B. Hendriks, J. Waelkens, J. M. Winne and F. E. Du Prez, *ACS Macro Lett.*, 2017, **6**, 930–934.

28 W. Denissen, G. Rivero, R. Nicolaÿ, L. Leibler, J. M. Winne and F. E. Du Prez, *Adv. Funct. Mater.*, 2015, **25**, 2451–2457.

29 Z. Ma, Y. Wang, J. Zhu, J. Yu and Z. Hu, *J. Polym. Sci., Part A: Polym. Chem.*, 2017, **55**, 1790–1799.

30 A. Ruiz de Luzuriaga, R. Martin, N. Markaide, A. Rekondo, G. Cabañero, J. Rodríguez and I. Odriozola, *Mater. Horiz.*, 2016, **3**, 241–247.

31 A. Ruiz De Luzuriaga, J. M. Matxain, F. Ruipérez, R. Martin, J. M. Asua, G. Cabañero and I. Odriozola, *J. Mater. Chem. C*, 2016, **4**, 6220–6223.

32 D. J. Fortman, R. L. Snyder, D. T. Sheppard and W. R. Dichtel, *ACS Macro Lett.*, 2018, **7**, 1226–1231.

33 D. J. Fortman, J. P. Brutman, C. J. Cramer, M. A. Hillmyer and W. R. Dichtel, *J. Am. Chem. Soc.*, 2015, **137**, 14019–14022.

34 R. L. Snyder, D. J. Fortman, G. X. De Hoe, M. A. Hillmyer and W. R. Dichtel, *Macromolecules*, 2018, **51**, 389–397.

35 A. Rekondo, R. Martin, A. Ruiz De Luzuriaga, G. Cabañero, H. J. Grande and I. Odriozola, *Mater. Horiz.*, 2014, **1**, 237–240.

36 B. Krishnakumar, R. V. S. Prasanna Sanka, W. H. Binder, C. Park, J. Jung, V. Parthasarthy, S. Rana and G. J. Yun, *Composites, Part B*, 2019, 107647.

37 J. Han, T. Liu, C. Hao, S. Zhang, B. Guo and J. Zhang, *Macromolecules*, 2018, **51**, 6789–6799.

38 J. J. Lessard, L. F. Garcia, C. P. Easterling, M. B. Sims, K. C. Bentz, S. Arencibia, D. A. Savin and B. S. Sumerlin, *Macromolecules*, 2019, **52**, 2105–2111.

39 M. Raimondo, C. Naddeo, L. Vertuccio, L. Bonnaud, P. Dubois, W. H. Binder, A. Sorrentino and L. Guadagno, *Nanotechnology*, 2020, **31**, 225708.

40 A. Romo-Uribe, J. A. Arcos-Casarrubias, A. Reyes-Mayer and R. Guardian-Tapia, *Polym.-Plast. Technol. Eng.*, 2017, **56**, 96–107.

41 W. S. Hummers and R. E. Offeman, *J. Am. Chem. Soc.*, 1958, **80**, 1339.

42 A. S. Nia, S. Rana, D. Döhler, X. Noirfalise, A. Belfiore and W. H. Binder, *Chem. Commun.*, 2014, **50**, 15374–15377.

43 N. M. Florea, A. Lungu, P. Badica, L. Craciun, M. Enculescu, D. G. Ghita, C. Ionescu, R. G. Zgirian and H. Iovu, *Composites, Part B*, 2015, **75**, 226–234.

44 N. Bosq, N. Guigo, J. Persello and N. Sbirrazzuoli, *Phys. Chem. Chem. Phys.*, 2014, **16**, 7830–7840.

45 C. Park, J. Jung and G. J. Yun, *Composites, Part B*, 2019, **161**, 639–650.

46 S. Kopsidas, V. G. Rocha, A. C. Taylor, S. Eslava, E. S. Gutierrez, A. J. Kinloch, G. B. Olowojoba and C. Mattevi, *J. Mater. Sci.*, 2017, **52**, 7323–7344.

47 F. E. Swallow, *J. Appl. Polym. Sci.*, 2002, **84**, 2533–2540.

48 C. Taplan, M. Guerre, J. M. Winne and F. E. Du Prez, *Mater. Horiz.*, 2020, **7**, 104–110.

49 M. Castelaín, P. S. Shuttleworth, C. Marco, G. Ellis and H. J. Salavagione, *Phys. Chem. Chem. Phys.*, 2013, **15**, 16806–16811.